SUPPORTING INFORMATION

For

Charge-Separation-Type Ionic Crystals with Mixed $Au^{I}_{4}Co^{III}_{2}$ and $Au^{I}_{4}Ni^{II}Co^{III}$ Hexanuclear Complexes

*Rycce S. Pratikha, Tatsuhiro Kojima, Naoto Kuwamura, Nobuto Yoshinari, and Takumi Konno**

Department of Chemistry, Graduate School of Science, Osaka University, Toyonaka, Osaka 560-0043, Japan

E-mail: konno@chem.sci.osaka-u.ac.jp

Table S1. Crystal data for $\mathbf{1}_{Li}$, $\mathbf{1}_{Na}$, $\mathbf{1}_{K}$, $\mathbf{1}_{Rb}$, and $\mathbf{1}_{Cs}$.

	$\mathbf{1}_{Li}$	$\mathbf{1}_{Na}$	$\mathbf{1}_{K}$	$\mathbf{1}_{Rb}$	$\mathbf{1}_{Cs}$
CCDC No.	1990698	1989961	1989962	1989963	1989964
Formula	$C_{72}H_{84}Au_4Co_{1.33}$ $N_6Ni_{0.67}O_{21.67}P_4S_4$	$C_{72}H_{84}Au_4Co_{1.33}$ $N_6Ni_{0.67}O_{21.67}P_4S_4$	$C_{72}H_{84}Au_4Co_{1.33}K_{0.67}$ $N_6Ni_{0.67}O_{21}P_4S_4$	$C_{72}H_{84}Au_4Co_{1.33}N_6$ $Ni_{0.67}O_{21}P_4Rb_{0.67}S_4$	$C_{72}H_{84}Au_4Co_{1.33}Cs_{0.67}$ $N_6Ni_{0.67}O_{20.67}P_4S_4$
Color, form	Purple, block	Purple, block	Purple, block	Purple, block	Purple, block
λ=Wavelength/ Å	0.4111	0.630	0.630	0.4248	0.630
Crystal system	Cubic	Cubic	Cubic	Cubic	Cubic
Space group	*F*23	*F*23	*F*23	*F*23	*F*23
a/ Å	37.528(2)	37.862(4)	37.923(4)	37.8088(13)	37.651(4)
b/ Å	37.528(2)	37.862(4)	37.923(4)	37.8088(13)	37.651(4)
c/ Å	37.528(2)	37.862(4)	37.923(4)	37.8088(13)	37.651(4)
α /°	90	90	90	90	90
β /°	90	90	90	90	90
γ /°	90	90	90	90	90
V/ Å^3	52852(10)	54276(19)	54539(19)	54048(6)	53374(17)
Z	24	24	24	24	24
T/ K	100(2)	100(2)	100(2)	100(2)	100(2)
F(000)	29424	29424	29600	29888	30112
ρ calcd / g· cm^{-3}	1.914	1.863	1.866	1.905	1.949
$\mu(\lambda)$/ mm^{-1}	1.745	5.147	4.965	1.948	5.236
Flack parameter	0.058(11)	0.009(4)	0.001(4)	0.004(5)	0.003(4)
Crystal size /mm^3	0.08×0.04×0.04	0.03×0.03×0.03	0.041×0.034×0.031	0.034×0.041×0.031	0.07×0.06×0.03
Limiting indices	$-48 \le h \le 48$	$-65 \le h \le 65$	$-45 \le h \le 46$	$-49 \le h \le 48$	$-51 \le h \le 51$
	$-48 \le k \le 47$	$-45 \le k \le 46$	$-64 \le k \le 65$	$-31 \le k \le 39$	$-51 \le k \le 51$
	$-47 \le l \le 48$	$-44 \le l \le 45$	$-45 \le l \le 43$	$-44 \le l \le 49$	$-60 \le l \le 51$
R1 (I>2σ(I))[a)]	0.0360	0.0554	0.0691	0.0212	0.0384
Rw2 (all data)[b)]	0.0891	0.1390	0.1737	0.0537	0.0870
GOF	1.038	1.063	1.109	1.077	0.925

Table S2. Crystal data for $\mathbf{1_{Ca}}$, $\mathbf{1_{Sr}}$, and $\mathbf{1_{Ba}}$.

	$\mathbf{1_{Ca}}$	$\mathbf{1_{Sr}}$	$\mathbf{1_{Ba}}$
CCDC No.	1989965	1989966	1989967
Formula	$C_{72}H_{84}Au_4Ca_{0.33}Co_{1.33}$ $N_{6.67}Ni_{0.67}O_{22}P_4S_4$	$C_{72}H_{84}Au_4Co_{1.33}N_{6.67}$ $Ni_{0.67}O_{22}P_4S_4Sr_{0.33}$	$C_{72}H_{84}Au_4Ba_{0.33}Co_{1.33}$ $N_{6.67}Ni_{0.67}O_{22}P_4S_4$
Color, form	Purple, block	Purple, block	Purple, block
λ=Wavelength/ Å	0.600	0.4248	0.630
Crystal system	Cubic	Cubic	Cubic
Space group	*F*23	*F*23	*F*23
a/ Å	37.650(2)	37.749(16)	37.910(4)
b/ Å	37.650(2)	37.749(16)	37.910(4)
c/ Å	37.650(2)	37.749(16)	37.910(4)
α /°	90	90	90
β /°	90	90	90
γ /°	90	90	90
V/ Å^3	53370(9)	53792(67)	54483(19)
Z	24	24	24
T/ K	100(2)	100(2)	100(2)
F(000)	29760	29904	30048
ρ calcd / g· cm^{-3}	1.916	1.913	1.901
$\mu(\lambda)$/ mm^{-1}	4.455	1.917	5.048
Flack parameter	0.004(4)	0.009(9)	0.004(3)
Crystal size /mm^3	0.06×0.04×0.04	0.06×0.05×0.04	0.064×0.055×0.045
Limiting indices	–59 ≤ h ≤ 57	–35 ≤ h ≤ 45	–45 ≤ h ≤ 44
	–59 ≤ k ≤ 59	–47 ≤ k ≤ 49	–64 ≤ k ≤ 65
	–57 ≤ l ≤ 55	–38 ≤ l ≤ 49	–43 ≤ l ≤ 44
R1 (I>2σ(I))[a)]	0.0372	0.0365	0.0562
Rw2 (all data)[b)]	0.0856	0.0834	0.1470
GOF	1.026	1.019	1.105

Table S3. Selected bond distances (Å) for $\mathbf{1}_{Li}$, $\mathbf{1}_{Na}$, $\mathbf{1}_{K}$, $\mathbf{1}_{Rb}$, and $\mathbf{1}_{Cs}$.

	$\mathbf{1}_{Li}$	$\mathbf{1}_{Na}$	$\mathbf{1}_{K}$	$\mathbf{1}_{Rb}$	$\mathbf{1}_{Cs}$
M-S/ Å	2.329(4)/2.356(3)	2.342(3)/2.356(3)	2.349(4)/2.375(3)	2.358(3)/2.373(3)	2.353(5)/2.360(5)
M-O/ Å	1.946(9)/1.970(8)	1.947(7)/1.967(7)	1.974(10)/1.974(9)	1.944(6)/1.997(6)	1.919(11)/1.998(10)
M-N/ Å	2.000(10)/2.007(11)	1.987(8)/1.995(8)	2.018(12)/2.022(12)	1.990(8)/2.016(8)	1.944(14)/1.991(13)

Table S4. Selected bond distances (Å) for $\mathbf{1}_{Ca}$, $\mathbf{1}_{Sr}$, and $\mathbf{1}_{Ba}$.

	$\mathbf{1}_{Ca}$	$\mathbf{1}_{Sr}$	$\mathbf{1}_{Ba}$
M-S/ Å	2.327(2)/2.348(2)	2.344(3)/2.366(3)	2.345(3)/2.362(3)
M-O/ Å	1.934(6)/1.963(6)	1.948(8)/1.974(8)	1.954(9)/1.976(7)
M-N/ Å	1.987(8)/1.995(8)	2.004(10)/2.023(10)	1.998(10)/2.019(11)

Preparation of $\mathbf{1_{Li}}$.

To a colorless solution of $[Au_2(dppe)(D\text{-}Hpen)_2]\cdot 8H_2O$ (0.10 g, 0.082 mmol) in methanol (16 mL) was added a pink methanol solution (16 mL) containing $Co(OAc)_2\cdot 4H_2O$ (0.011 g, 0.046 mmol) and $Ni(OAc)_2\cdot 4H_2O$ (0.011 g, 0.046 mmol). After stirring at room temperature for 3 h in air, the solution turned brown. Subsequently, a 0.5 M $LiNO_3$ aqueous solution (1.5 mL) was added to the brown solution. Slow evaporation of the solution at room temperature for 7 days gave a mixture of purple block crystals ($\mathbf{1_{Li}}$) and green needle crystals (**2**). Purple crystals of $\mathbf{1_{Li}}$ were obtained as a pure product from the mixture by dissolving **2** using a mixture of methanol and H_2O.

Yield for $\mathbf{1_{Li}}$: 71 mg (66%). Anal. Calc for $(H_3O)_{0.67}[Au_4Ni_{0.67}Co_{1.33}(dppe)_2(D\text{-}pen)_4](NO_3)_2\cdot 10H_2O$ = $C_{72}H_{106.01}Au_4Co_{1.33}N_6Ni_{0.67}O_{24.67}P_4S_4$: C, 33.16; H, 4.10; N, 3.22%. Found: C, 33.20; H, 4.03; N, 3.14%. IR spectrum (cm^{-1}, ATR): 1653/1604 (ν_{COO-}), 1105 ($\nu_{P\text{-}Ph}$), 735-692 (ν_{Ph}) and 1350 (ν_{NO3-}). The yield of **2** was estimated to be 16 % based on the weight loss after dissolving **2**.

X-ray crystallography of $\mathbf{1_{Li}}$.

The diffraction data for $\mathbf{1_{Li}}$ were recorded at 100 K with a PILATUS3 X CdTe 1M with synchrotron radiation (λ = 0.4111 Å) at SPring-8 (BL02B1 beamline). The diffraction images were processed by using RAPID-AUTO. The structures were solved by direct methods using SHELXS-2014. The structure refinements were carried out using full-matrix least-squares (SHELXL-2018/3).

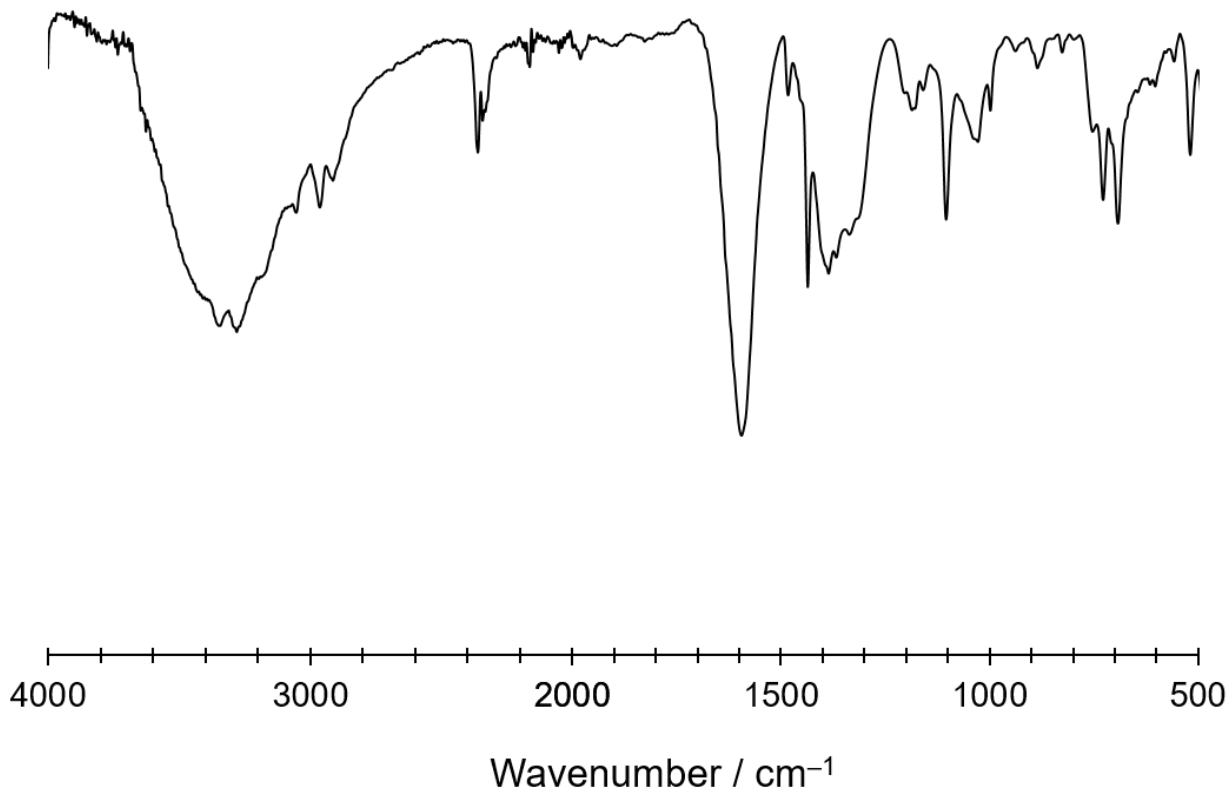

Figure S1. IR spectrum (ATR) of **2**.

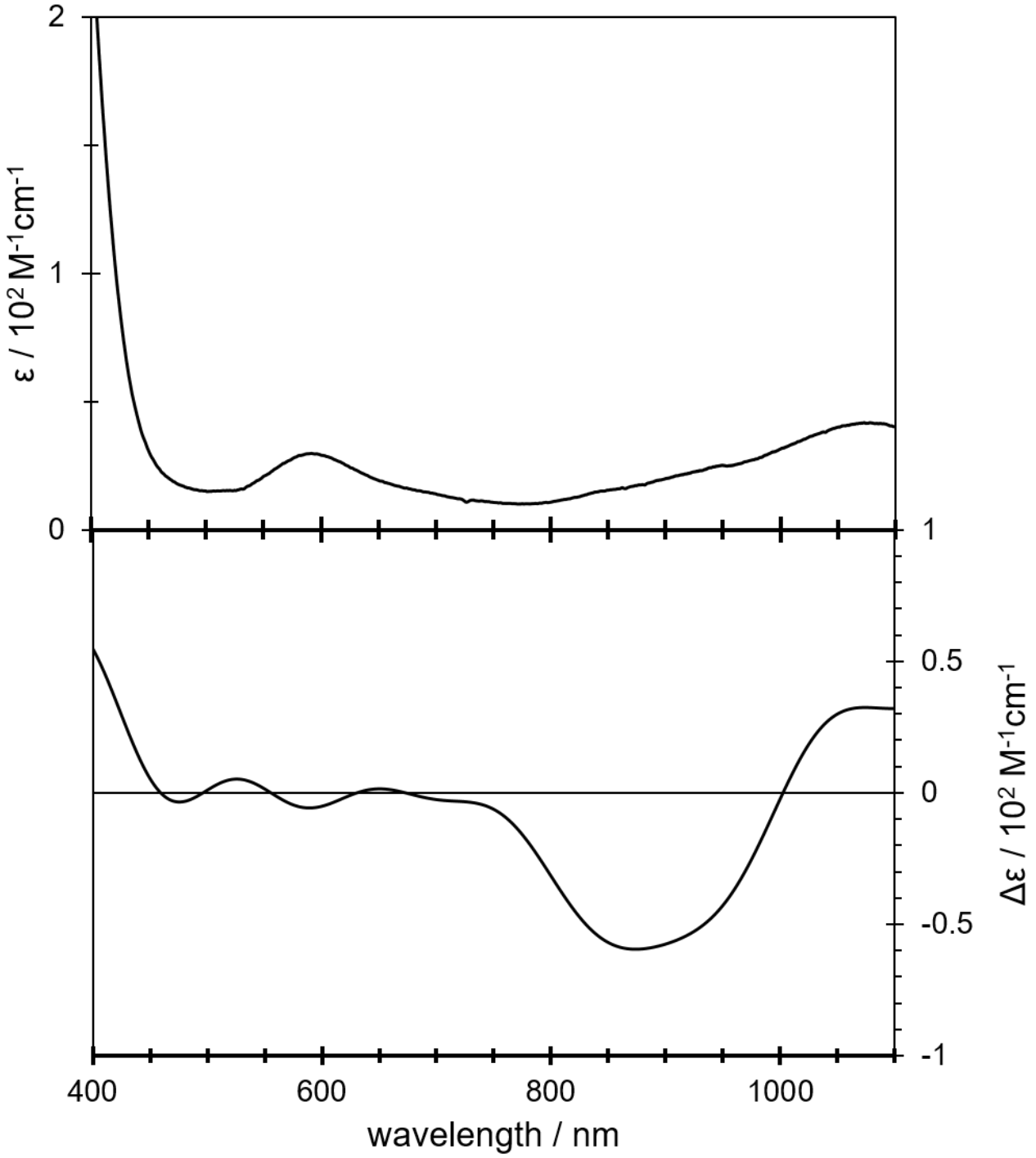

Figure S2. Absorption (top) and CD (bottom) spectra of **2** in methanol.

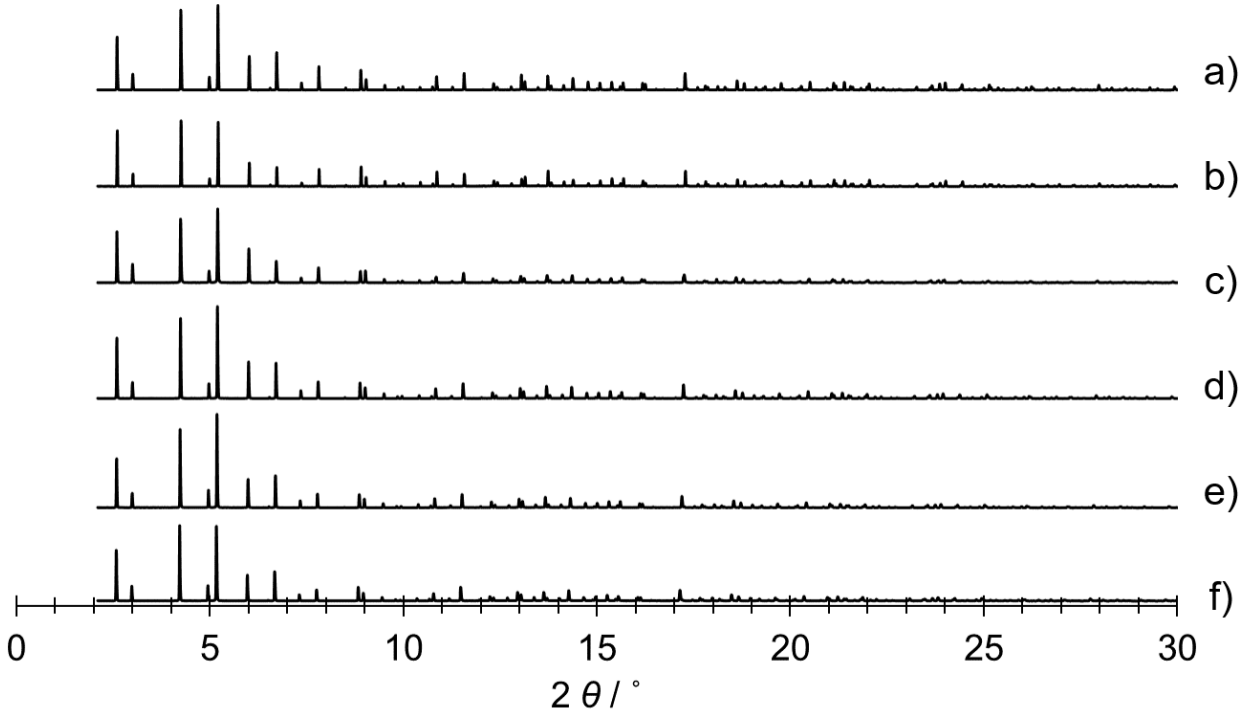

Figure S3. PXRD patterns (λ = 1.000 Å). a) $[Co^{III}_2(L^{Au})_2](NO_3)_2$, b) $\mathbf{1}_{\mathbf{Li}}$, c) $\mathbf{1}_{\mathbf{Na}}$, d) $\mathbf{1}_{\mathbf{K}}$, e) $\mathbf{1}_{\mathbf{Rb}}$, and f) $\mathbf{1}_{\mathbf{Cs}}$.

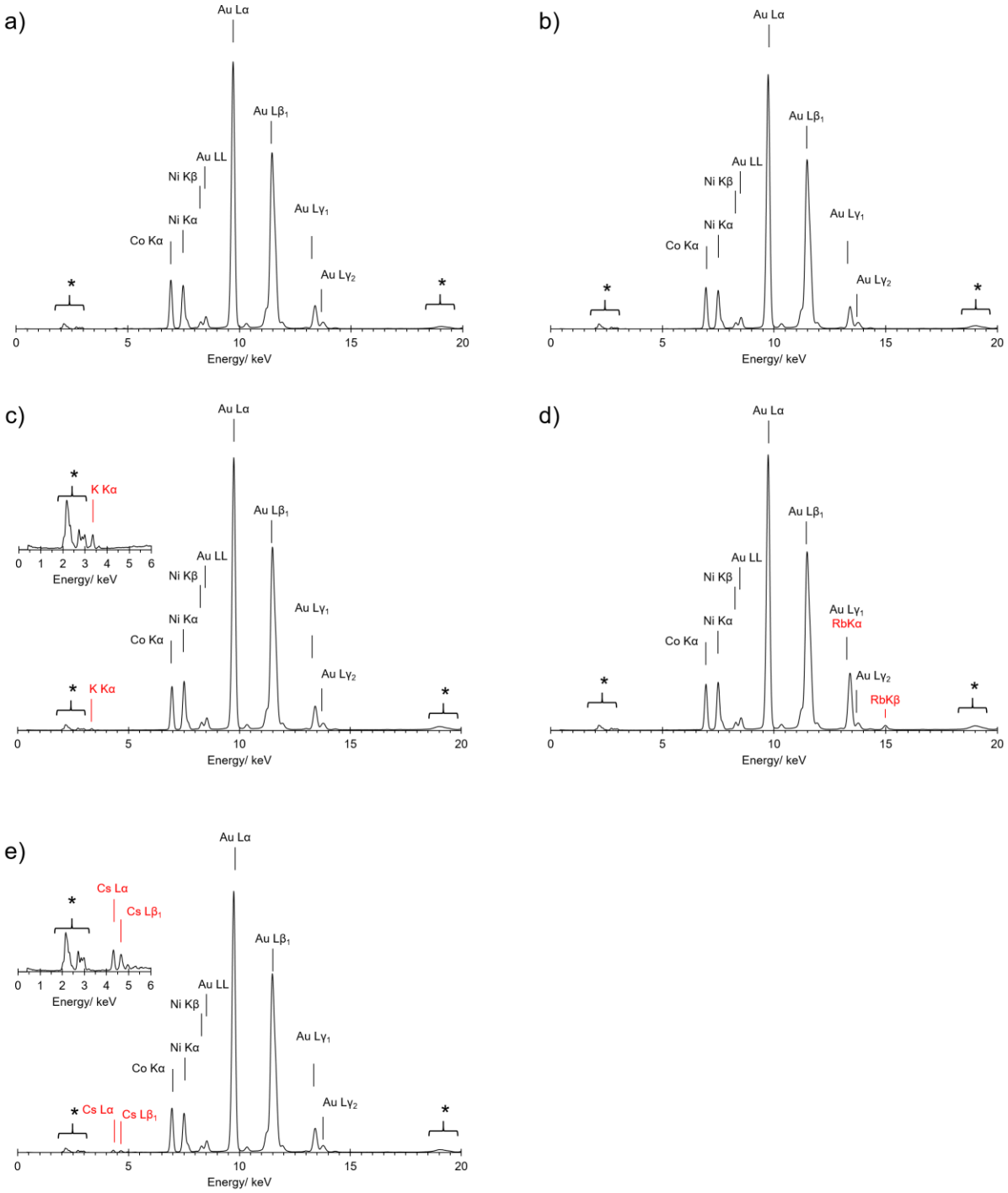

Figure S4. X-ray fluorescence spectra of a) $\mathbf{1}_{\mathbf{Li}}$, b) $\mathbf{1}_{\mathbf{Na}}$, c) $\mathbf{1}_{\mathbf{K}}$, d) $\mathbf{1}_{\mathbf{Rb}}$, and e) $\mathbf{1}_{\mathbf{Cs}}$. * represents signals from the X-ray tube. The inset represents the magnified spectrum (0~6 keV).

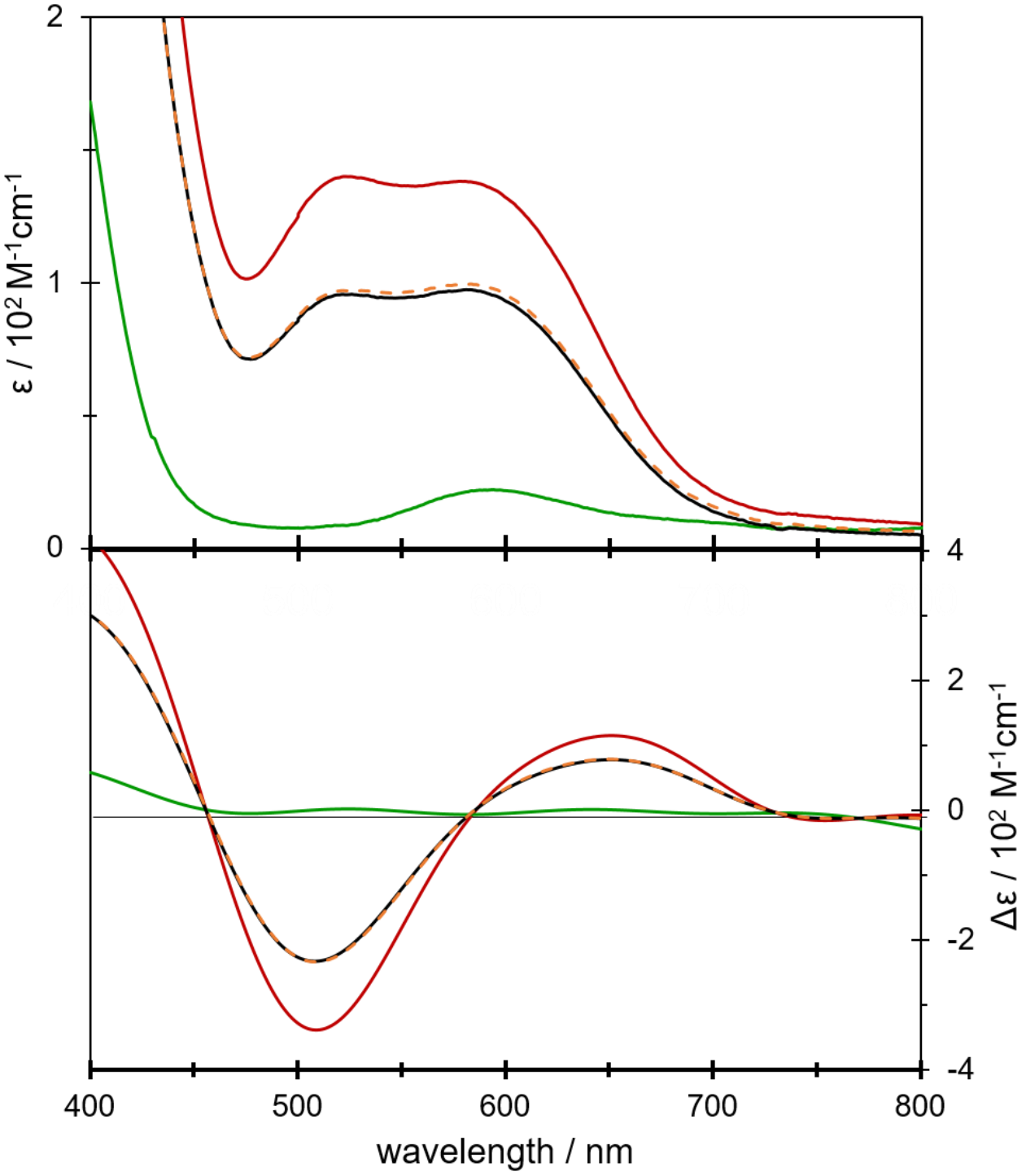

Figure S5. Absorption (top) and CD (bottom) spectra in methanol: black line; $\mathbf{1}_{\mathbf{Na}}$, red line; $[Co^{III}_2(L^{Au})_2](NO_3)_2$, green line; $[Ni^{II}_2(L^{Au})_2]$, orange broken line; a mixture of $[Ni^{II}_2(L^{Au})_2]$ and $[Co^{III}_2(L^{Au})_2](NO_3)_2$ in a 1:2 ratio.

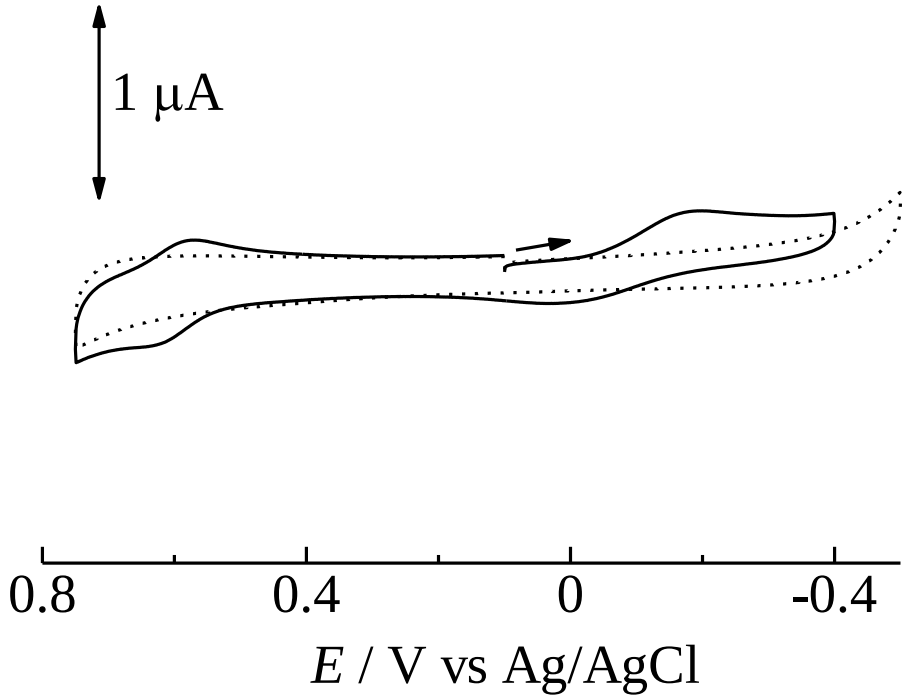

Figure S6. Cyclic voltammograms of $\mathbf{1}_{Na}$ (solid line) and blank (dotted line) in MeOH containing 0.1 M $NaBF_4$ with a scan rate of 30 mV/sec.

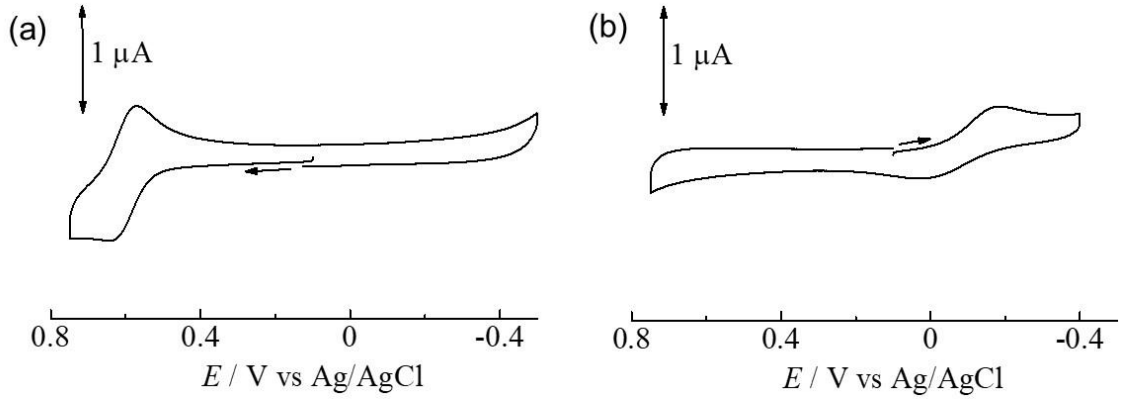

Figure S7. Cyclic voltammograms of $[Ni^{II}_2(L^{Au})_2]$ (a) and $[Co^{III}_2(L^{Au})_2](NO_3)_2$ (b) in MeOH containing 0.1 M $NaBF_4$ with a scan rate of 30 mV/sec.

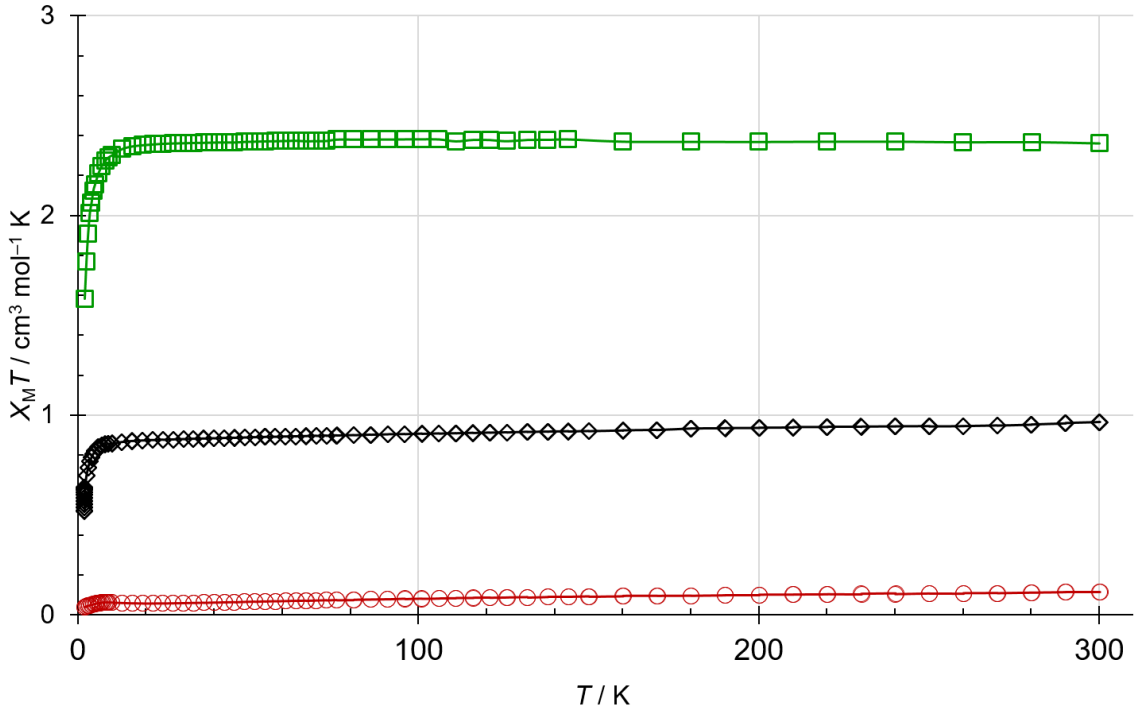

Figure S8. The $\chi_M T$ vs T plots for $\mathbf{1}_{\mathbf{Na}}$ (black), $[Ni^{II}_2(L^{Au})_2]$ (green), and $[Co^{III}_2(L^{Au})_2](NO_3)_2$ (red).

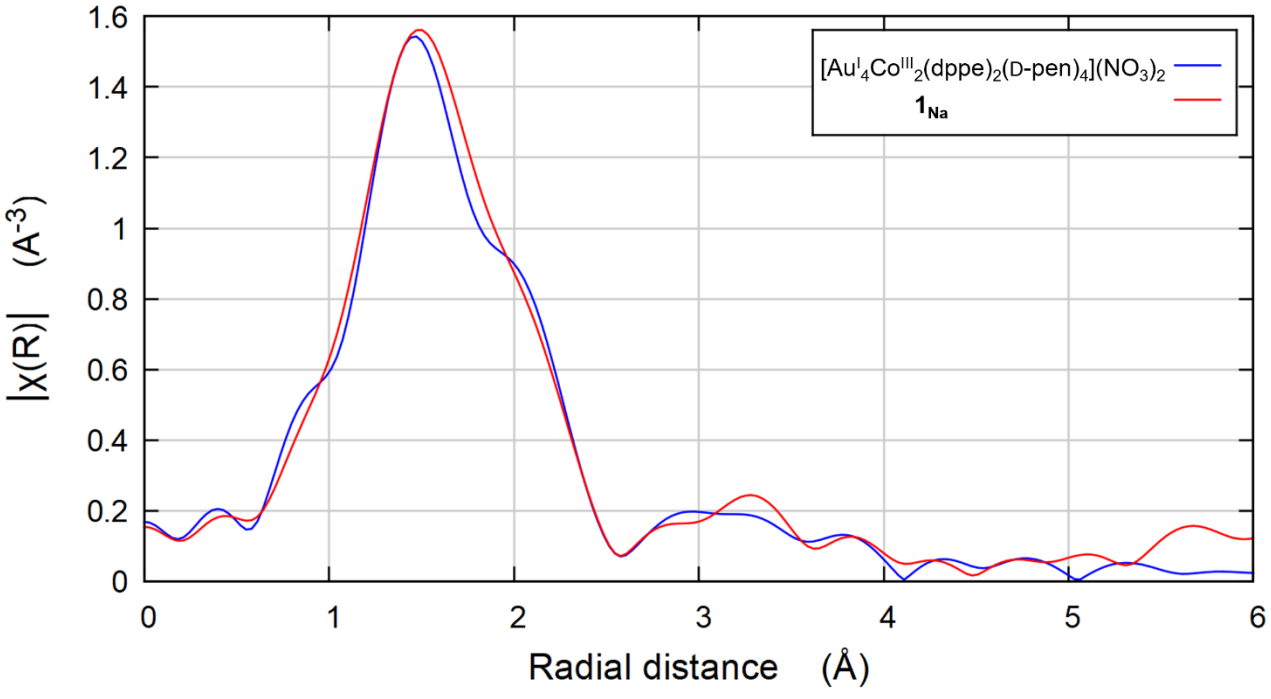

Figure S9. Fourier transforms of the Co K-edge EXAFS of $\mathbf{1}_{\mathbf{Na}}$ (red line) and $[Co^{III}_2(L^{Au})_2](NO_3)_2$ (blue line).

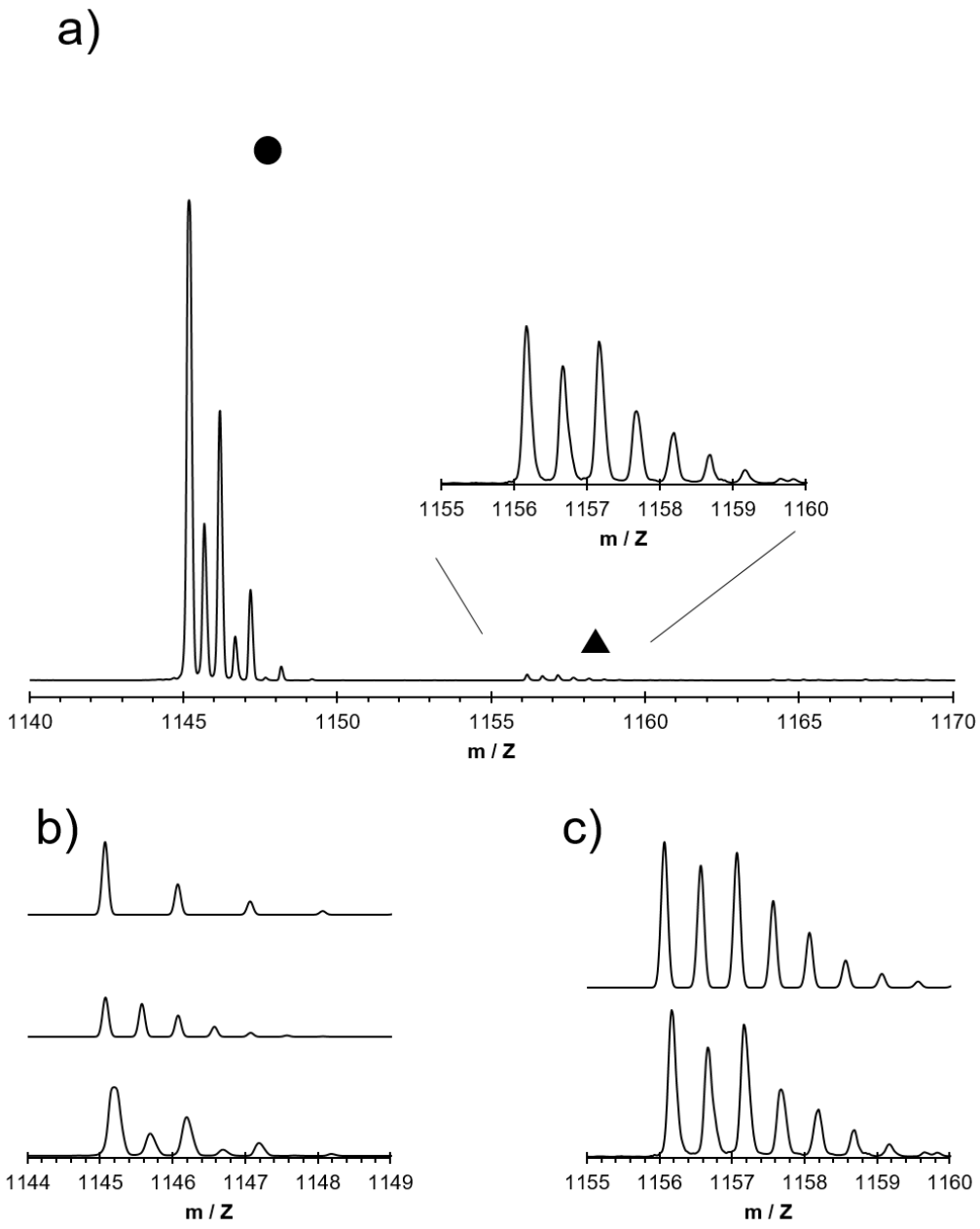

Figure S10. a) ESI mass spectrum of $\mathbf{1_{Na}}$ in MeOH (positive mode). b) The observed (bottom) and simulated isotope patterns for $[Au^{I}_2Co^{III}(dppe)(D\text{-pen})_2]^+$ (top) and $[Au^{I}_4Co^{III}_2(dppe)_2(D\text{-pen})_4]^{2+}$ (middle) at m/Z = 1145.2 (●). c) The observed (bottom) and simulated (top) isotope patterns for $\{[Au^{I}_4Ni^{II}Co^{III}(dppe)_2(D\text{-pen})_4] + Na\}^{2+}$ at m/Z = 1156.2 (▲).

The observed pattern at m/Z = 1145.2 (●) for $\mathbf{1_{Na}}$ matches well with the simulated pattern of a 2:1 mixture of the trinuclear $[Au^{I}_2Co^{III}(dppe)(D\text{-pen})_2]^+$ and the hexanuclear $[Au^{I}_4Co^{III}_2(dppe)_2(D\text{-pen})_4]^{2+}$, indicative of the equilibrium between the trinuclear and the hexanuclear structures in solution for $[Au^{I}_4Co^{III}_2(dppe)_2(D\text{-pen})_4]^{2+}$.

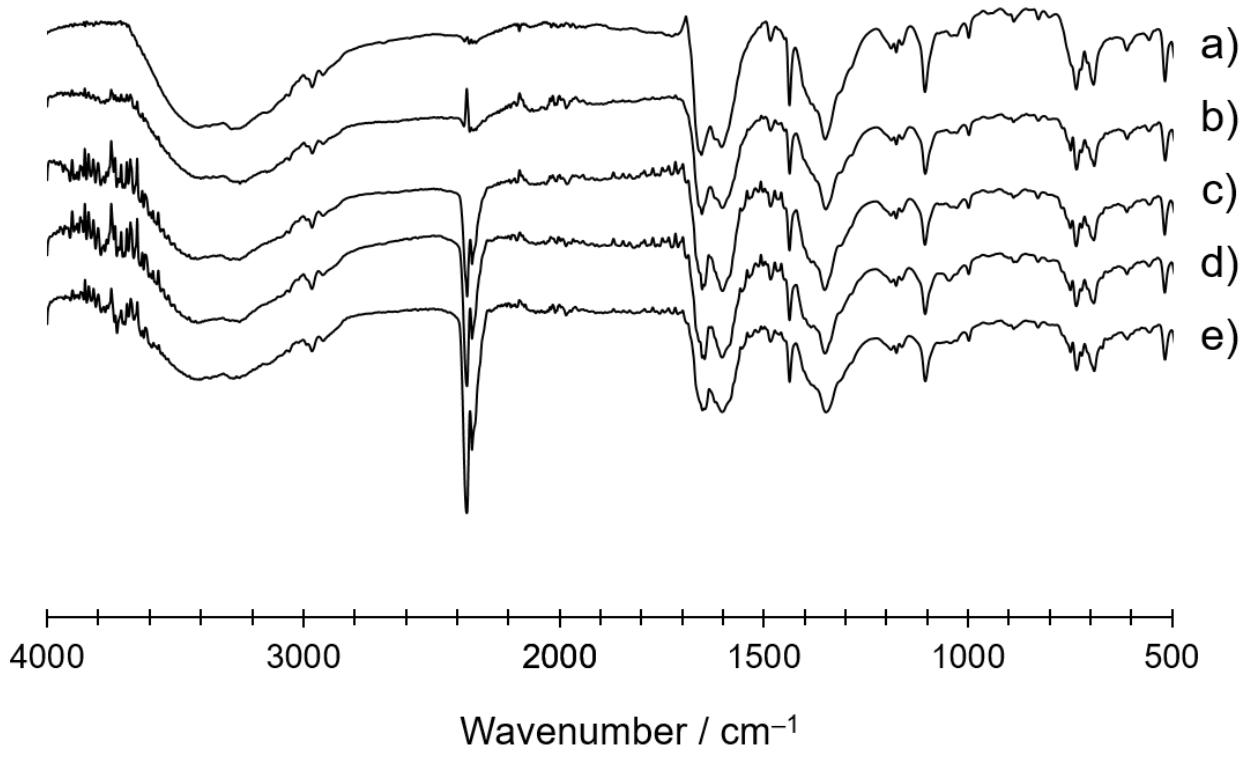

Figure S11. IR spectra (ATR): a) $\mathbf{1}_{\mathbf{Li}}$, b) $\mathbf{1}_{\mathbf{Na}}$, c) $\mathbf{1}_{\mathbf{K}}$, d) $\mathbf{1}_{\mathbf{Rb}}$, and e) $\mathbf{1}_{\mathbf{Cs}}$.

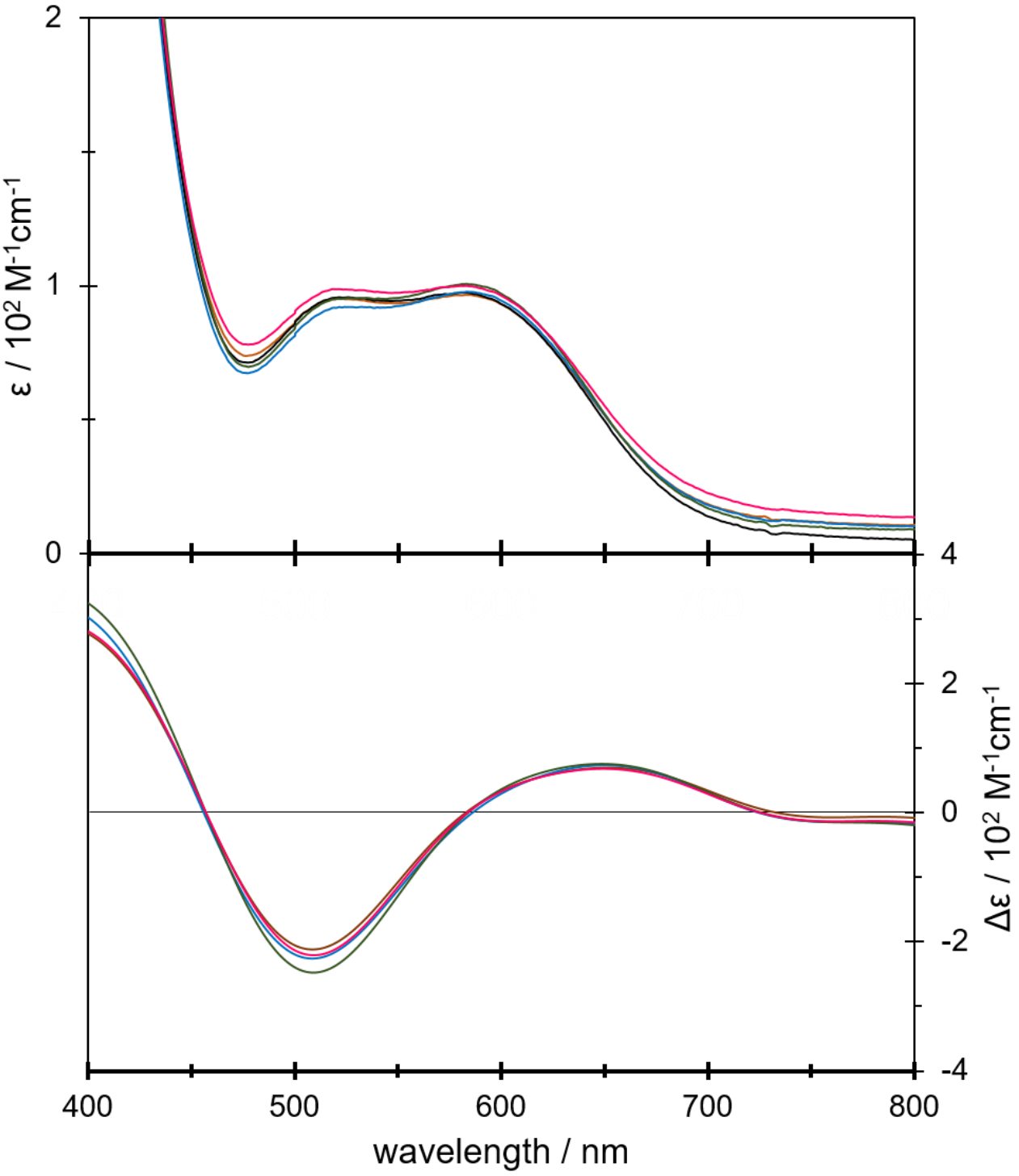

Figure S12. Absorption (top) and CD (bottom) spectra in methanol: brown; $\mathbf{1}_{Li}$, black; $\mathbf{1}_{Na}$, blue; $\mathbf{1}_{K}$, green; $\mathbf{1}_{Rb}$, pink; $\mathbf{1}_{Cs}$.

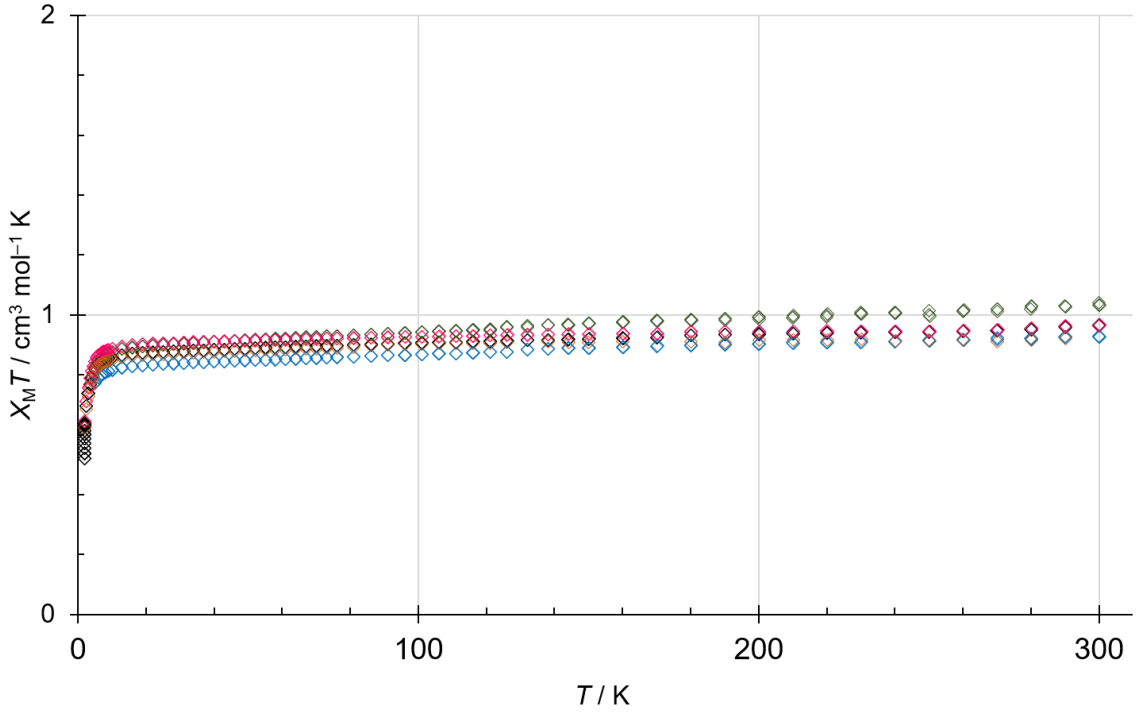

Figure S13. The $\chi_M T$ vs T plots: brown; **1**$_{Li}$, black; **1**$_{Na}$, blue; **1**$_{K}$, green; **1**$_{Rb}$, pink; **1**$_{Cs}$.

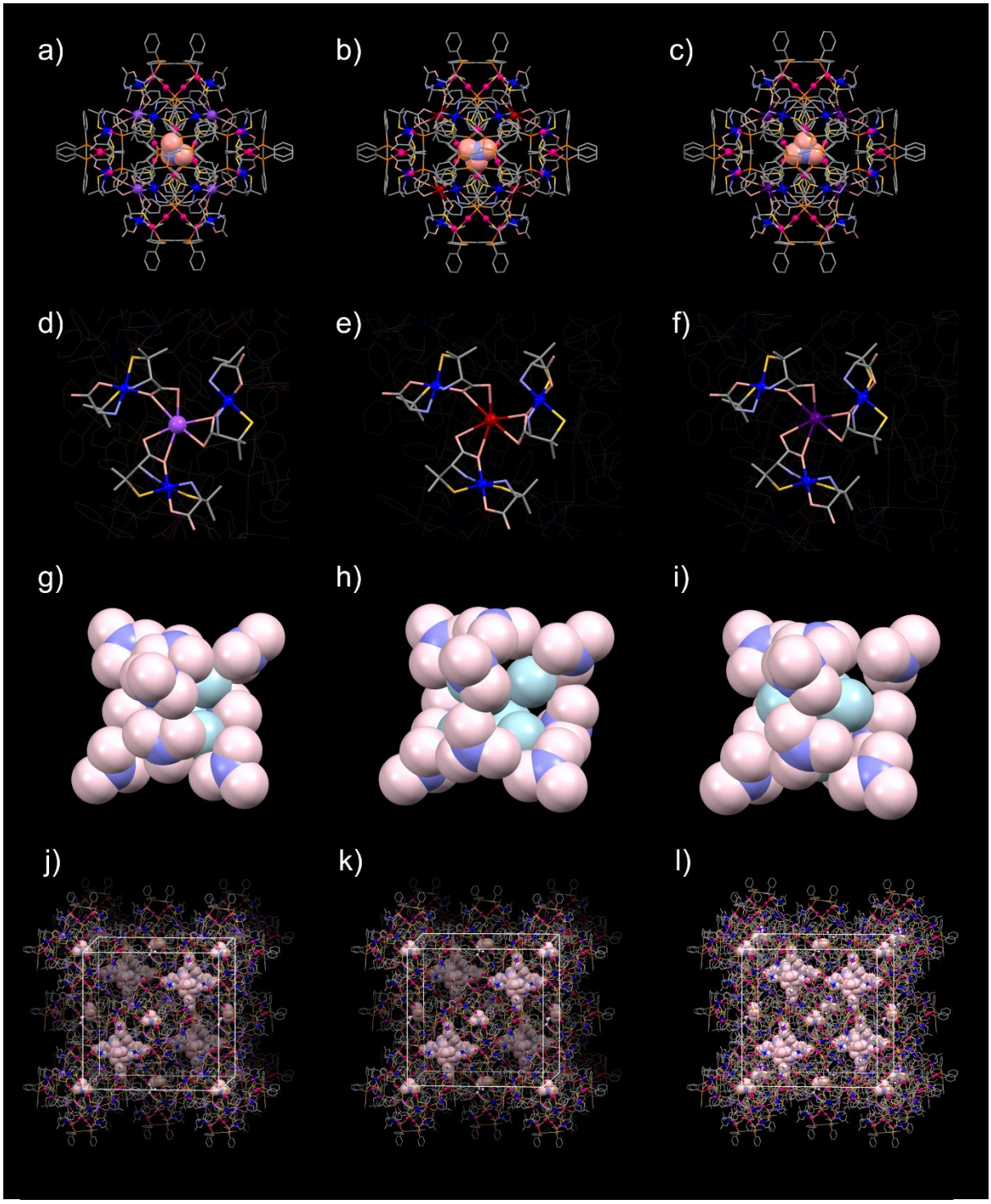

Figure S14. Crystal structures of $\mathbf{1}_{K}$, $\mathbf{1}_{Rb}$, and $\mathbf{1}_{Cs}$. Cationic supramolecular octahedra in $\mathbf{1}_{K}$ (a), $\mathbf{1}_{Rb}$ (b) and $\mathbf{1}_{Cs}$ (c). M^{1} ion surrounded by D-pen carboxylate groups in $\mathbf{1}_{K}$ (d), $\mathbf{1}_{Rb}$ (e) and $\mathbf{1}_{Cs}$ (f). Adamantane-like nitrate cluster in $\mathbf{1}_{K}$ (g), $\mathbf{1}_{Rb}$ (h) and $\mathbf{1}_{Cs}$ (i). Packing structure of $\mathbf{1}_{K}$ (j), $\mathbf{1}_{Rb}$ (k) and $\mathbf{1}_{Cs}$ (l). Nitrate anions are represented by a space-filling model. Color codes: red, Au; blue, Co/Ni; orange, P; yellow, S; pink/light pink, O; pale blue, N; gray, C; purple, K; brown, Rb; violet, Cs.

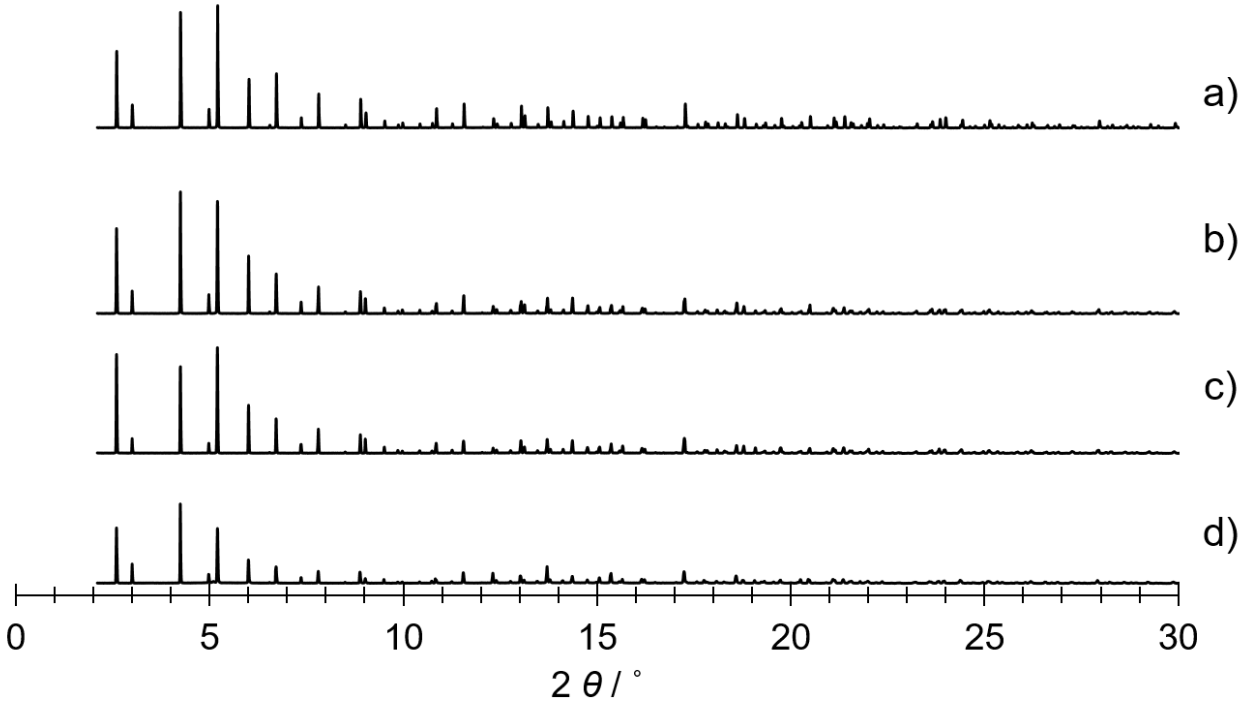

Figure S15. PXRD patterns (λ = 1.000 Å). a) $[Co^{III}_2(L^{Au})_2](NO_3)_2$, b) **1**$_{Ca}$, c) **1**$_{Sr}$, and d) **1**$_{Ba}$.

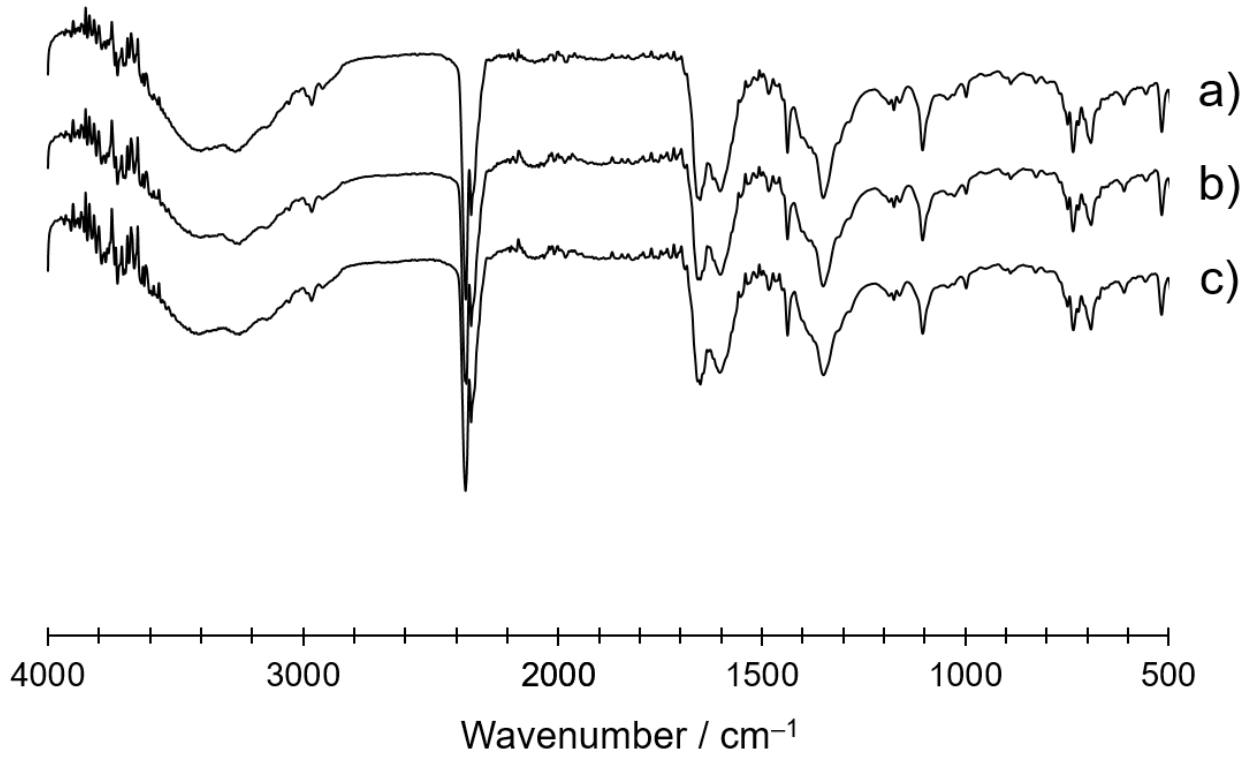

Figure S16. IR spectra (ATR): a) $\mathbf{1}_{Ca}$, b) $\mathbf{1}_{Sr}$, and c) $\mathbf{1}_{Ba}$.

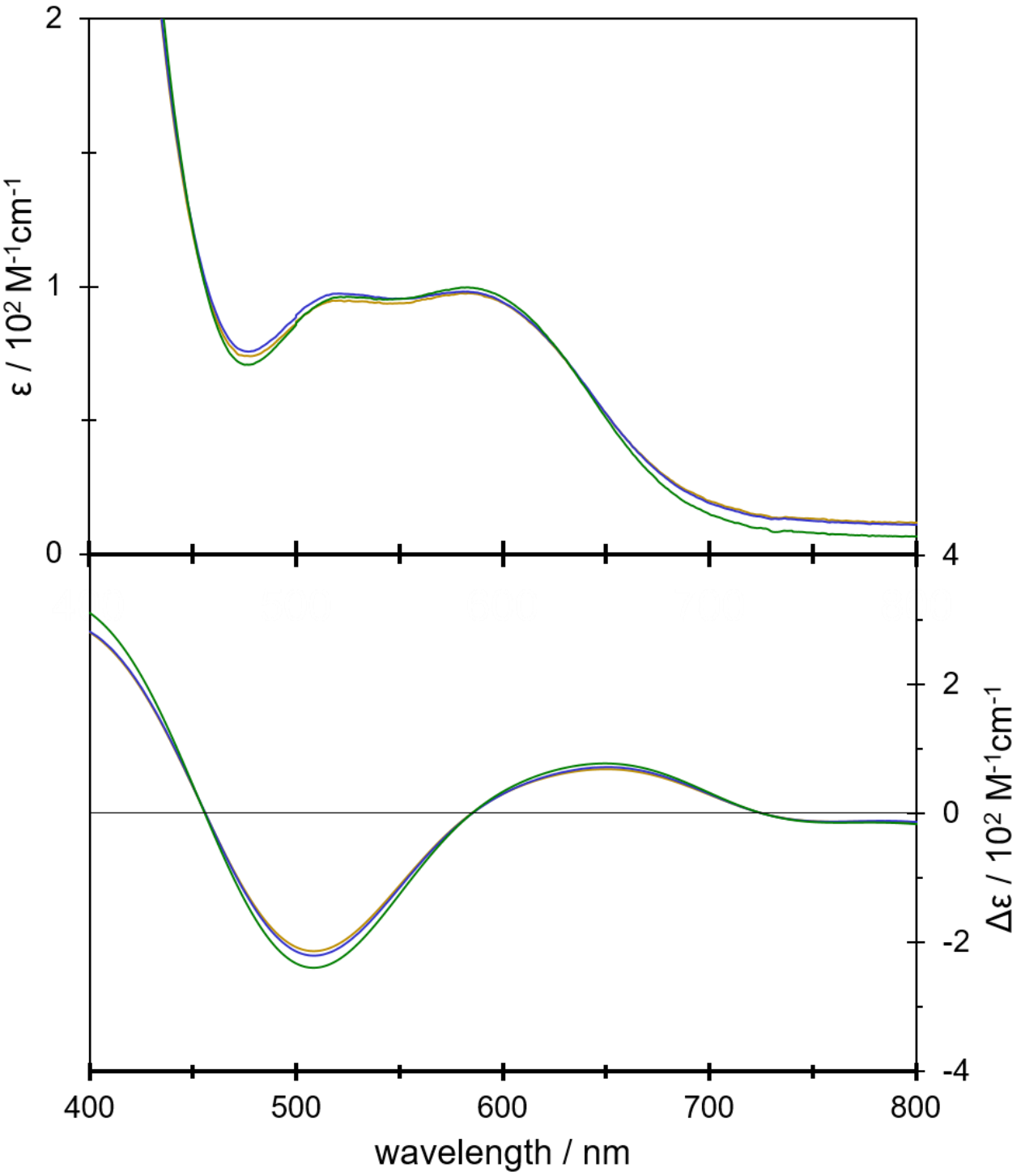

Figure S17. Absorption (top) and CD (bottom) spectra in methanol: yellow; $\mathbf{1}_{Ca}$, blue; $\mathbf{1}_{Sr}$, and green; $\mathbf{1}_{Ba}$.

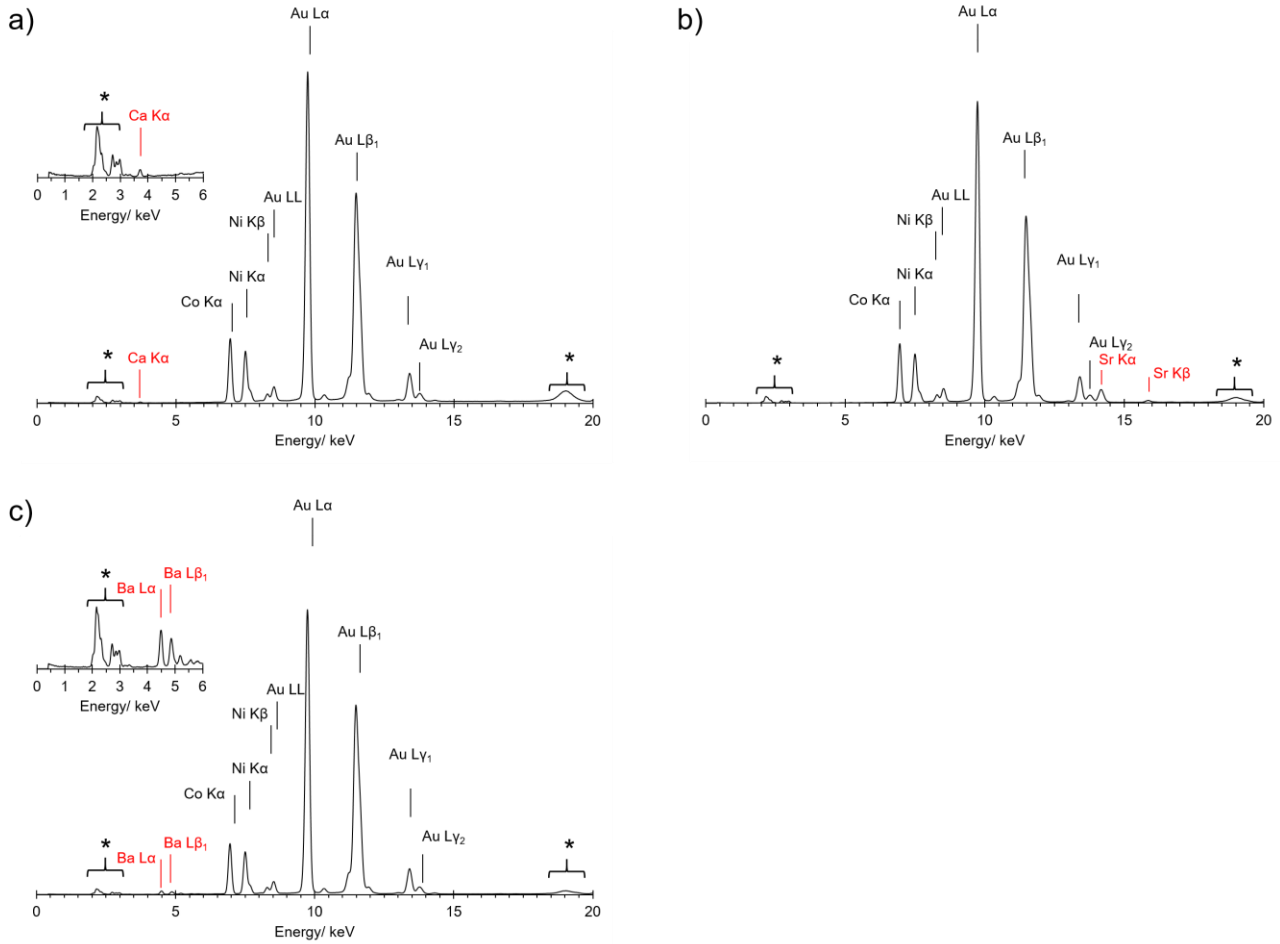

Figure S18. X-ray fluorescence spectra of a) $\mathbf{1}_{Ca}$, b) $\mathbf{1}_{Sr}$, and c) $\mathbf{1}_{Ba}$. * represents signals from the X-ray tube. The inset represents the magnified spectrum (0~6 keV).

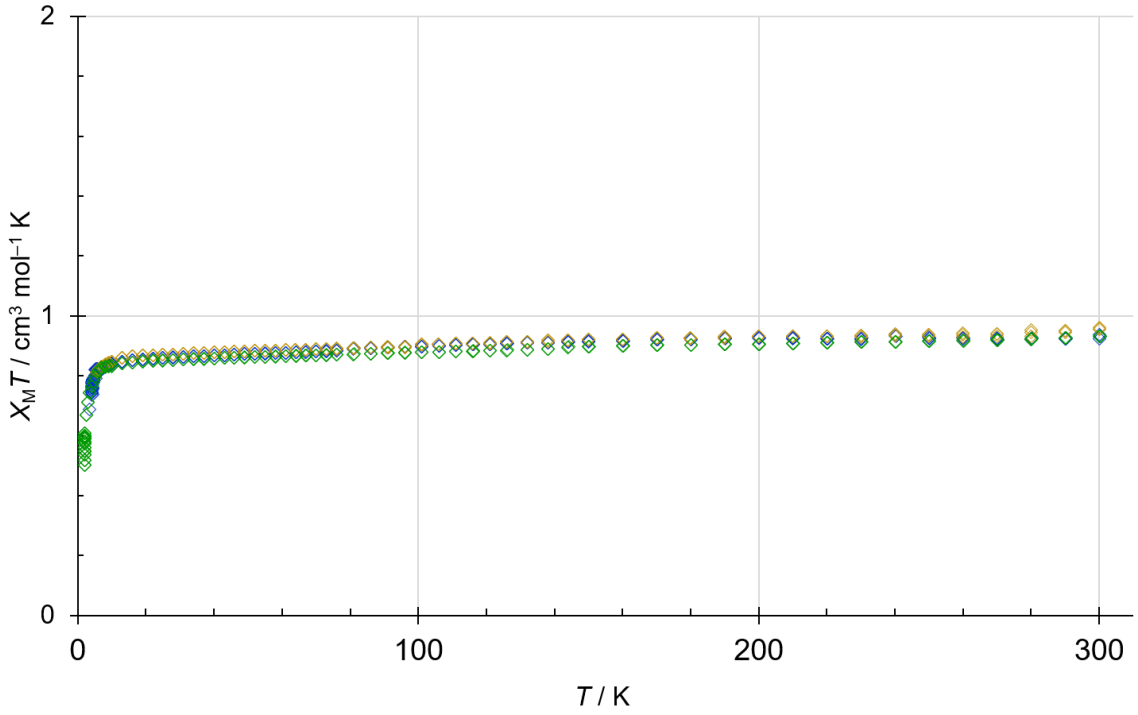

Figure S19. The $\chi_M T$ vs T plots: yellow; **1**$_{Ca}$, blue; **1**$_{Sr}$, and green; **1**$_{Ba}$.

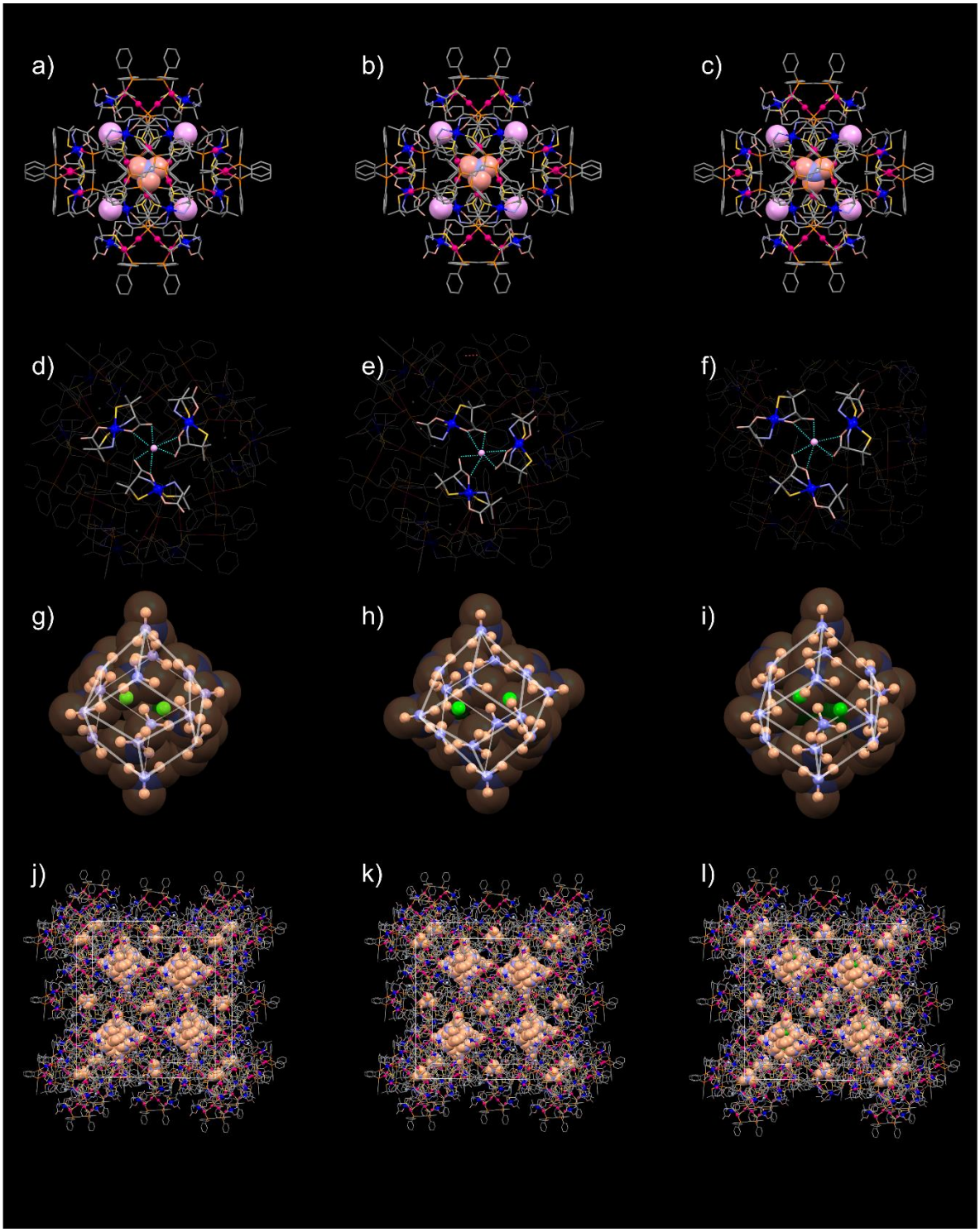

Figure S20. Crystal structures of $\mathbf{1}_{Ca}$, $\mathbf{1}_{Sr}$, and $\mathbf{1}_{Ba}$. Cationic supramolecular octahedra in $\mathbf{1}_{Ca}$ (a), $\mathbf{1}_{Sr}$ (b), and $\mathbf{1}_{Ba}$ (c). H_3O^+ ions are surrounded by D-pen carboxylate groups in $\mathbf{1}_{Ca}$ (d), $\mathbf{1}_{Sr}$ (e), and $\mathbf{1}_{Ba}$ (f). Rhombic dodecahedron-like nitrate cluster in $\mathbf{1}_{Ca}$ (g), $\mathbf{1}_{Sr}$ (h), and $\mathbf{1}_{Ba}$ (i). Packing structure of $\mathbf{1}_{Ca}$ (j), $\mathbf{1}_{Sr}$ (k), and $\mathbf{1}_{Ba}$ (l). Nitrate anions are represented by a space-filling model. Color codes: red, Au; blue, Co/Ni; orange, P; yellow, S; pink/light orange, O; pale blue, N; gray, C; green, Ca/Sr/Ba.

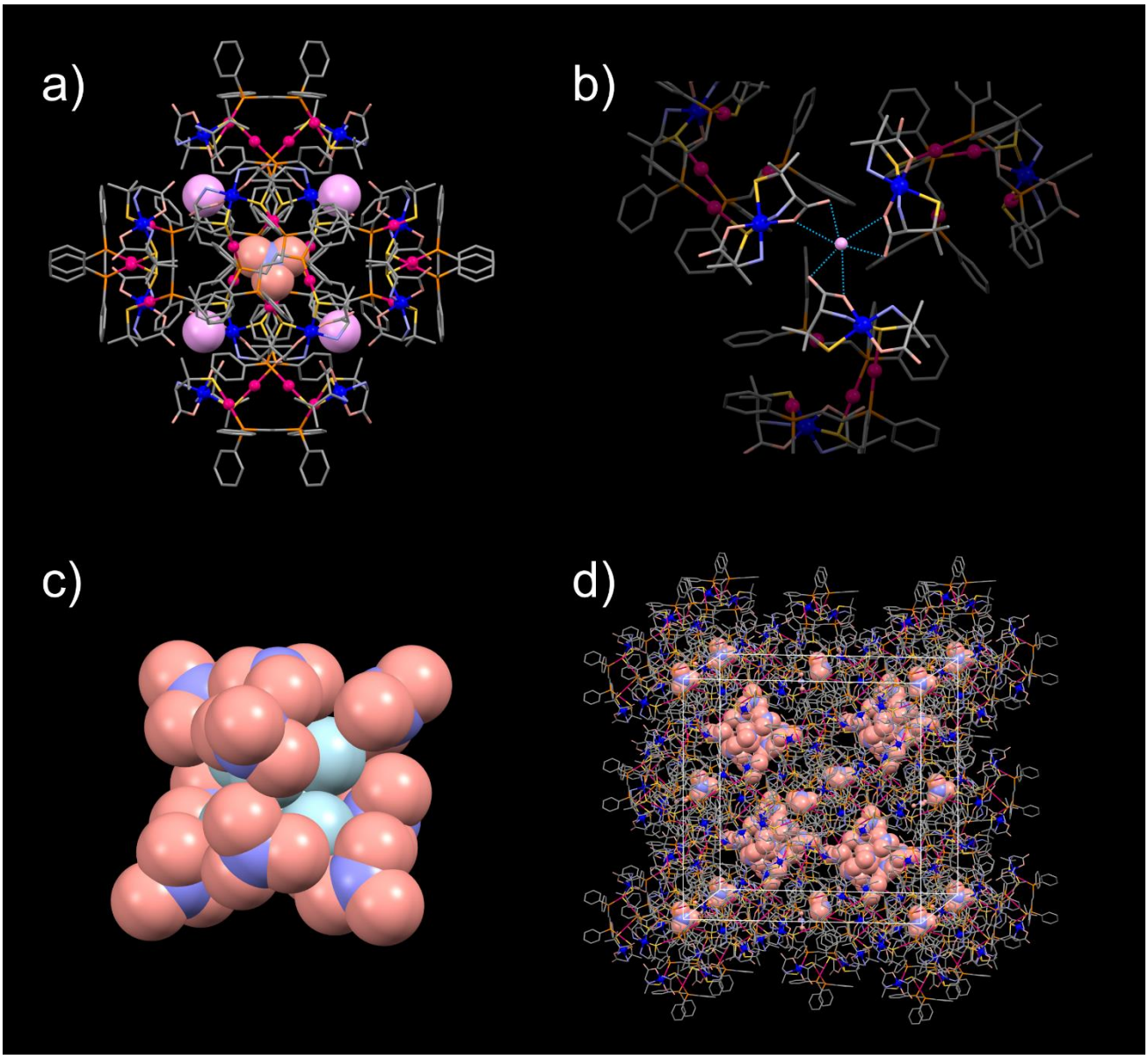

Figure S21. Crystal structure of $\mathbf{1}_{\mathbf{Li}}$. (a) Cationic supramolecular octahedron. (b) H_3O^+ ion surrounded by D-pen carboxylate groups. (c) Adamantane-like nitrate cluster. (d) Packing structure. Nitrate anions are represented by a space-filling model. Color codes: red, Au; blue, Co/Ni; orange, P; yellow, S; pink/light blue, O; pale blue, N; gray, C; light pink, H_3O^+.